Fracture Analysis of the Heat-Affected Zone in the NESC-1 Spinning Cylinder Experiment[1]

J. A. Keeney
Oak Ridge National Laboratory,
P. O. Box 2009,
Oak Ridge, TN, 37831-8056

This paper presents updated analyses of the cylinder specimen being used in the international Network for Evaluating Steel Components (NESC) large-scale spinning-cylinder project (NESC-1). The NESC was organized as an international forum to exchange information on procedures for structural integrity assessment, to collaborate on specific projects, and to promote the harmonization of international standards. The objective of the NESC-1 project is to focus on a complete procedure for assessing the structural integrity of aged reactor pressure vessels. A clad cylinder containing through-clad and subclad cracks will be tested under pressurized-thermal shock conditions at AEA Technology, Risley, U.K. Three-dimensional finite-element analyses were carried out to determine the effects of including the cladding heat-affected zone (HAZ) in the models. The cylinder was modeled with inner-surface through-clad cracks having a depth of 74 mm and aspect ratios of 2:1 and 6:1. The cylinder specimen was subjected to centrifugal loading followed by a thermal shock and analyzed with a thermoelastic-plastic material model. The peak K_I values occurred at the clad/HAZ interface for the 6:1 crack and at the HAZ/base interface for the 2:1 crack. The analytical results indicate that cleavage initiation is likely to be achieved for the 6:1 crack, but questionable for the 2:1 crack.

Introduction

In recent years, several international collaborative programs have been initiated to evaluate and exchange knowledge and capabilities in specific disciplines that support pressure vessel and piping integrity assessments. The Network for Evaluating Steel Components (NESC), managed by the Commission of the European Communities, was organized as an international forum to exchange information on procedures for structural integrity assessment, to collaborate on specific projects, and to promote the harmonization of international standards. The initial project proposed by the NESC is designed to study the entire procedure of structural integrity assessments of aged reactor pressure vessels (RPVs) containing subclad cracks. In this project, important safety assessment issues will be investigated by means of inspection and analysis of a large-scale spinning cylinder with thermal-shock loading (NESC-1). The loading conditions of the cylinder simulate pressurized-thermal shock loading of an RPV in a loss-of-coolant accident.

Updated design analyses of the NESC-1 specimen were performed in response to a request from the NESC Project Management. Previous analyses (Keeney, 1994) indicated that cleavage initiation of a deep through-clad crack is likely to be achieved for initial and coolant temperatures of 295 and 5°C, respectively, but the cylinder models contained only base and clad materials. The Oak Ridge National Laboratory (ORNL) was requested to assist the NESC Task Group on Analysis to determine the predicted effect of including the clad heat-affected zone (HAZ) in the cylinder model. The cladding HAZ varies from 5 to 10 mm in thickness and is tougher than the base metal. This paper presents results from three-dimensional (3-D) finite-element analyses of the cylinder specimen being used in the NESC-1 project.

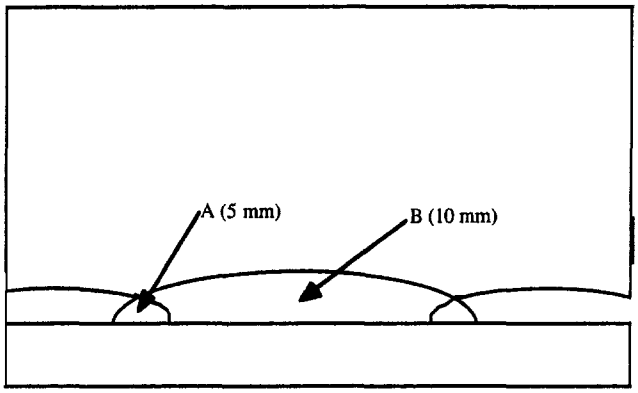

Fig. 1 Structure of the clad HAZ

Problem Definition

The cylinder specimen utilized in the analyses for NESC-1 has an inner diameter of 1045 mm, a wall thickness (including the cladding and clad HAZ) of 175 mm, clad thickness of 4 mm, and length of 1296 mm. The cylinder was fabricated from A508B class 3 steel with a clad overlay of 308 stainless steel. Metallographic sectioning of the clad test block revealed that the HAZ is a distinctive layer below the cladding with a periodicity associated with the width of the cladding pass of ≈60 mm (McAllister, 1996). Some overlap of these cladding passes was observed such that there was some tempering of the previous HAZ strip at its extremities. The resultant appearance of the HAZ is shown in Fig. 1. The depth of the HAZ layer in the tempered zone A was measured to be ≈5 mm, while the depth at *B* was measured at 10 mm. The best (obtainable) representative material properties are given in Table 1. These properties were provided by the NESC Task Group on Analysis and Task Group

[1] Research Sponsored by the Office of Nuclear Regulatory Research, U.S. Nuclear Regulatory Commission under Interagency Agreement 1886-8663-1W with the U.S. Department of Energy under Contract DE-AC05-96OR22464 with Lockheed Martin Energy Research Corp.

Contributed by the Pressure Vessels and Piping Division and presented at the Pressure Vessels and Piping Conference, Orlando, Florida, July 27–31, 1997, of THE AMERICAN SOCIETY OF MECHANICAL ENGINEERS. Manuscript received by the PVP Division, August 12, 1997; revised manuscript received April 15, 1998. Associate Technical Editor: M. B. Ruggles.

Table 1 Material properties for NESC-1 analyses

Material Property	A508 Base Forging	HAZ	Stainless Steel Cladding
Thermal Conduct. (k), W/m•K	33.92	33.92	15.30
Specific Heat (c_p), J/kg•K	541	541	495
Density (ρ), kg/m^3	7787	7787	7920
Young's Modulus (E), GPa	212.35 @ 0°C 189.10 @ 350°C	212.35 @ 0°C 189.10 @ 350°C	200.00 @ 20°C 178.00 @ 288°C
Coefficient of Thermal Expansion (α), per °C	1.186E-05@ 0°C 1.340E-05@350°C	1.186E-05@ 0°C 1.340E-05@350°C	1.389E-05@ 20°C 1.850E-05@288°C
Poisson's Ratio (ν)	0.28	0.28	0.30
Yield Stress (σ_y), MPa	527.9 @ 20°C 460.9 @ 150°C	648.4 @ 20°C 499.8 @ 150°C	179.6 @ 27°C 44.16 @ 288°C

Heat transfer coefficient : 22,000 W/m^2•K (inner surface)

on Materials. Note that the yield stress (tensile property) for the HAZ is much higher than that of the base metal.

Analyses were carried out for two inner-surface through-clad cracks with a crack depth of 74 mm and aspect ratios (crack length to crack depth) of 6:1 and 2:1. The loading conditions in the analyses consisted of the cylinder being heated to an initial temperature (T_i) of 295°C, spun at increasing speed (maximum acceleration is 180 rpm/min) about its axial centerline up to a maximum speed of 2500 rpm, and then thermally shocked on the inner surface with coolant at a temperature (T_c) of 5°C to achieve cleavage crack initiation. The analytical results were compared with material fracture toughness data taken from Lacey et al. (1991) and Bass (1996) to predict whether the crack would initiate. Figure 2 shows the upper and lower bounds of toughness plotted against temperature from the compact tension (CT) specimen data and an estimated toughness for the SC-4 test result. The toughness data for SC-4 are shown as a straight line due to the uncertainty in temperature at the crack tip at initiation (Lacey et al., 1991). The Materials Task Group has determined that the fracture toughness of the base metal is approximately the same as SC-4 (Bass, 1996). Also shown in Fig. 2 is an estimated toughness curve for the HAZ. The fracture toughness of the HAZ is higher than that of the base metal, i.e., for a fracture toughness of 100 MPa$\sqrt{m}$, the reference temperature for the HAZ is 16°C and for the base metal, 65°C (Bass, 1996).

Fracture Analysis

Heat Conduction Model. The calculation of the temperature distribution in the NESC-1 cylinder was performed with the ABAQUS (1996) finite-element program (a nuclear quality assurance certified (NQA-1) code) using an axisymmetric model. The model consisted of 21 nodes and 10 axisymmetric

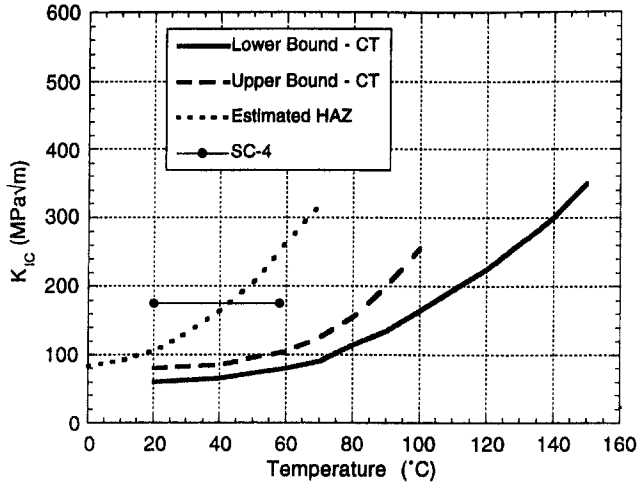

Fig. 2 Fracture toughness data for small-scale CT specimens, HAZ, and SC-4

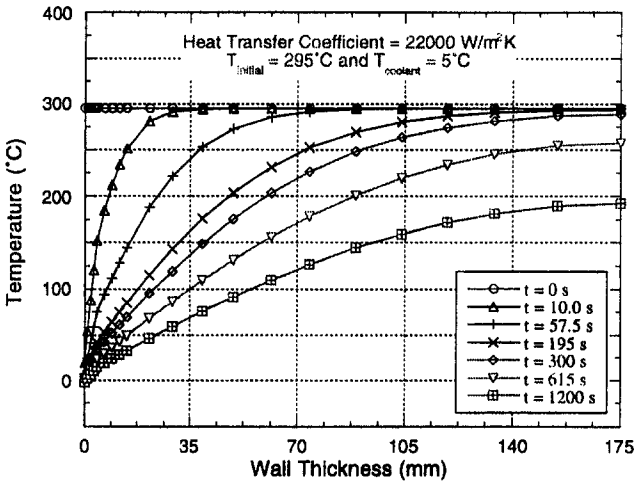

Fig. 3 Radial temperature distribution in the cylinder wall calculated by ABAQUS

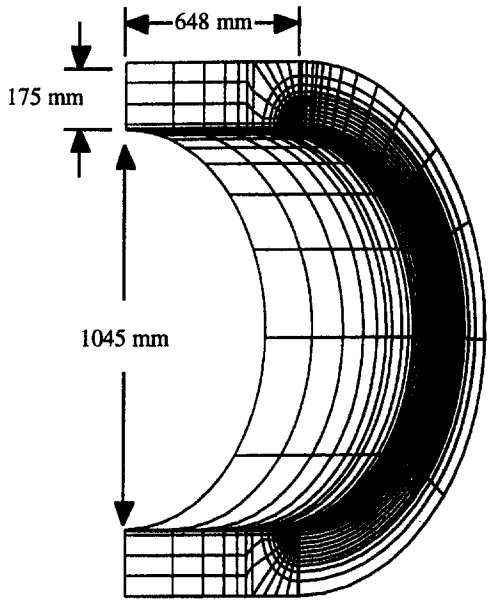

Fig. 4 Three-dimensional finite-element model of the clad cylinder (NESC-1) with a 74-mm-deep through-clad crack and 2:1 aspect ratio

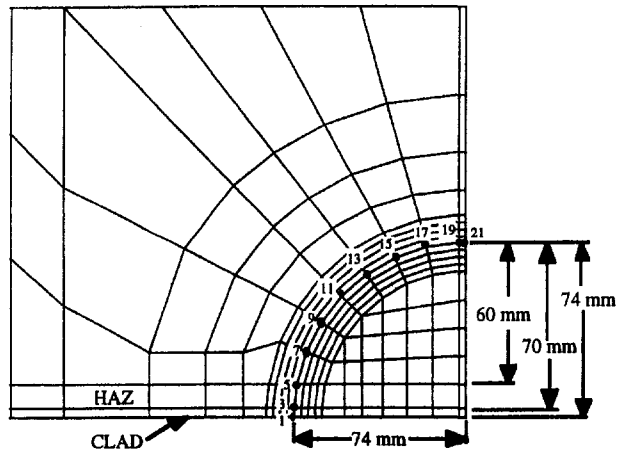

(*a*) 2:1 aspect ratio

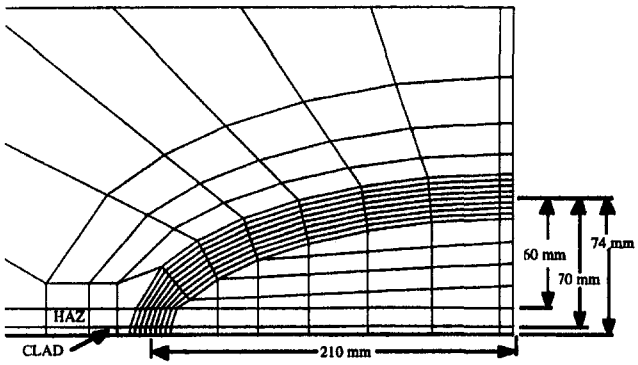

(*b*) 6:1 aspect ratio

Fig. 5 Crack-tip region of the cylinder model

one-dimensional (1-D) conduction elements with convection boundary conditions. The geometry, material properties, and loading conditions were summarized in the previous section. Figure 3 shows the calculated temperature distribution in the cylinder wall for different time steps.

3-D Finite-Element Model. Two models with through-clad semielliptical axial cracks at the inner surface having aspect ratios of 6:1 and 2:1 and a crack depth of 74 mm were evaluated in this study. The clad HAZ thickness used in these models is

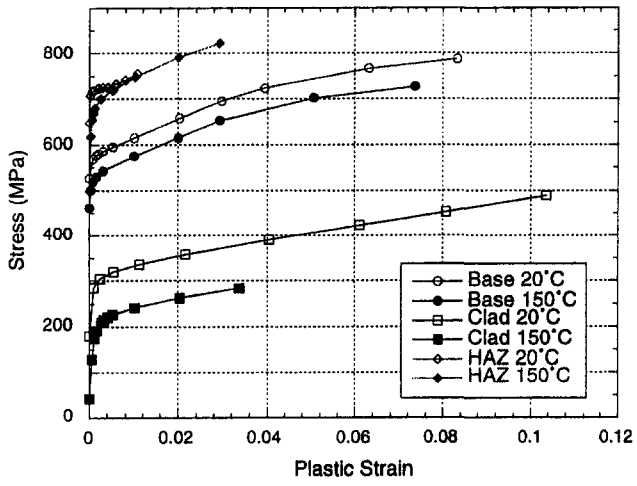

Fig. 6 Multilinear representations of the stress-plastic strain behavior for A508B base forging, 308 stainless steel clad, and HAZ materials

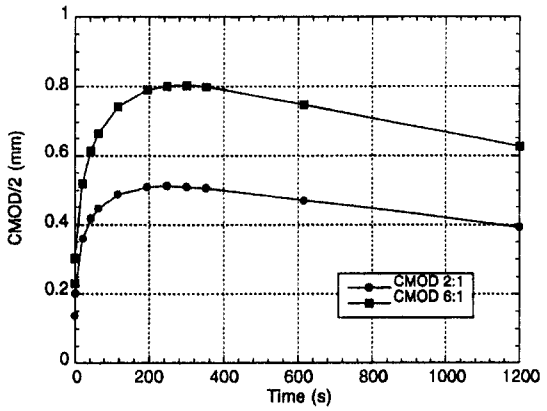

Fig. 7 Comparison of calculated CMOD curves for the two aspect ratios

10 mm. Comparable models are being generated and analyzed at Vattenfall Ringhals (Sweden) with an HAZ thickness of 5 mm. The 3-D finite-element model of the cylinder was generated with the ORMGEN (Bass and Bryson, 1982) mesh-generating program. From symmetry conditions, only one-fourth of the cylinder (180 deg model) is included in the model (Figs. 4 and 5). Both models consist of 10792 nodes and 2255 20-noded isoparametric elements. Detailed plots of the crack-tip regions for both models are shown in Fig. 5.

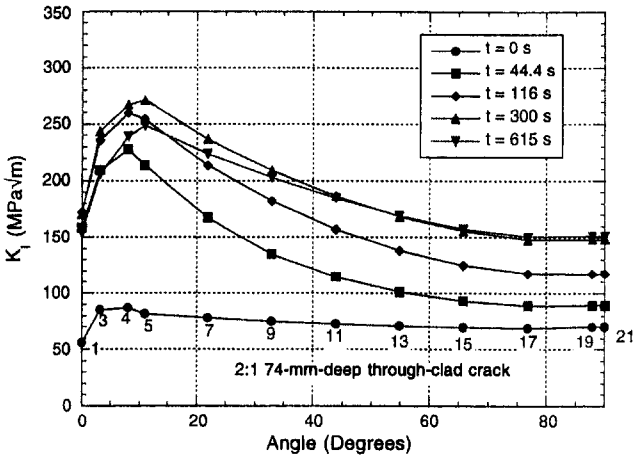

(*a*) The peak K_I value is at the HAZ/base interface for the crack with the 2:1 aspect ratio

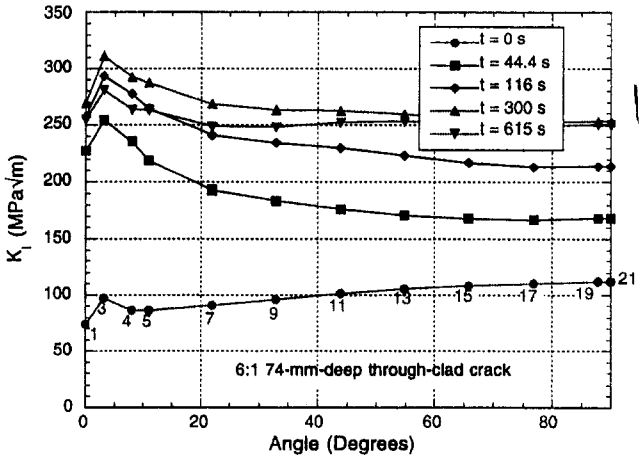

(*b*) The peak K_I value is at the clad/HAZ interface for the crack with the 6:1 aspect ratio

Fig. 8 Comparison of K_I values

The cylinder was analyzed with the ABAQUS (1996) finite-element program, which employs a domain integral method for the computation of the J-integral. The K_I value was calculated from the J-integral using the following plane-strain relation:

$$K = \sqrt{JE/(1 - \nu^2)} \quad (1)$$

where E = 189.1 GPa and ν = 0.28 for the base and HAZ materials, and E = 178.0 GPa and ν = 0.30 for the clad material. The thermoelastic-plastic analyses were performed using the material properties in Table 1 and the stress-plastic strain curves depicted in Fig. 6. The temperatures through the wall for each time step were obtained from the heat conduction analysis and were applied to the cylinder by interpolation. The "stress-free" temperature was taken as the initial temperature (prior to thermal shock) of the cylinder (residual stress effects were ignored).

CMOD and K_I Evaluation. Crack-mouth opening displacement (CMOD) was calculated for both crack geometries (aspect ratios of 2:1 and 6:1). As shown in Fig. 7, which plots CMOD/2 versus time, the peak CMOD value is 37 percent higher for the 6:1 crack than the 2:1 crack. K_I was calculated at nodal positions along the crack front. Values are plotted as functions of time and angle in Figs. 8(a) and (b) for the 2:1 and 6:1 models, respectively. In Fig. 9, K_I values are plotted as a function of time for positions 3, 4, and 5 around the crack front; see Fig. 5(a) for these locations. The peak K_I value for the 2:1 crack is at the HAZ/base interface (position 5) at a time of 300 s. For the 6:1 crack, the peak K_I value is at the clad/HAZ interface (position 3) at a time of 300 s.

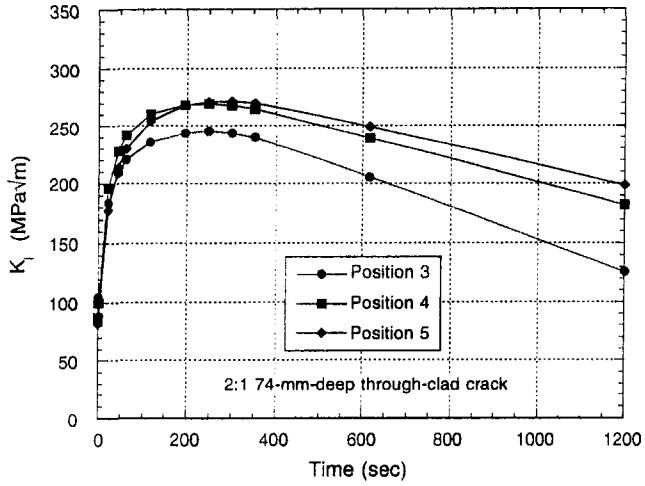

(a) 2:1 aspect ratio

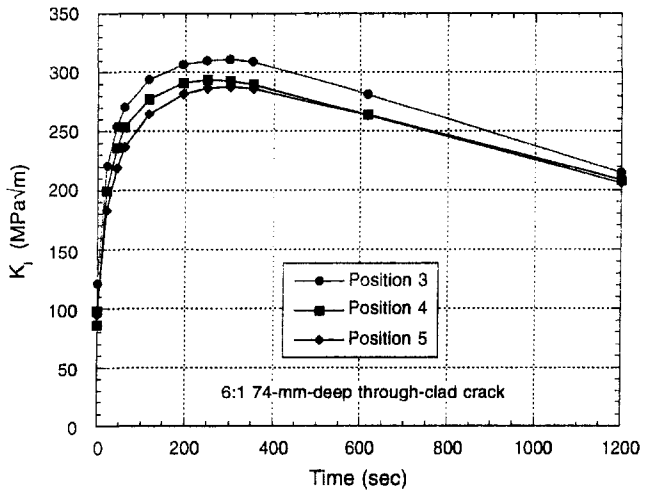

(b) 6:1 aspect ratio

Fig. 9 The highest K_I value is at a time of 300 s

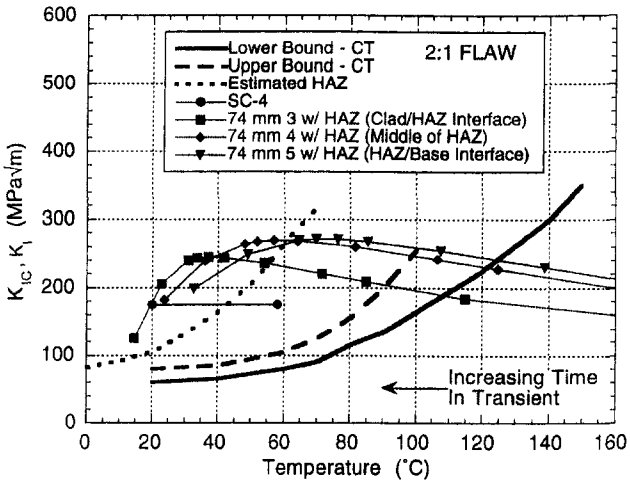

(a) 2:1 aspect ratio

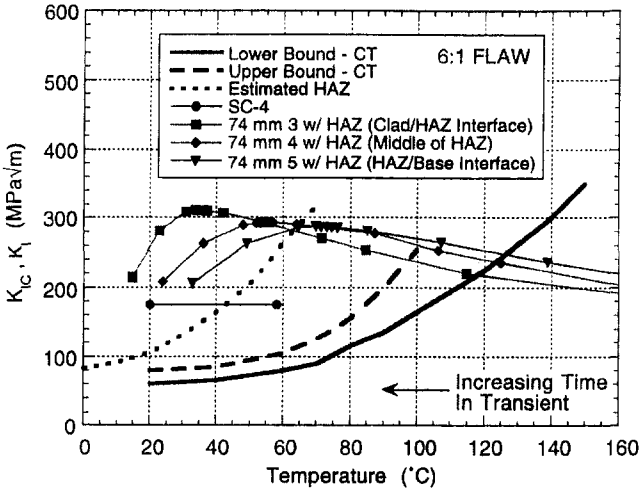

(b) 6:1 aspect ratio

Fig. 10 Comparison of K_I values with material toughness

In Fig. 10, values of K_I for the same positions around the crack front (as in Fig. 9) are plotted as a function of temperature and compared with the fracture toughness values from Fig. 2. For the 2:1 crack, Fig. 10(a), the peak K_I values occurred at the HAZ/base interface; but $\dot{K}$ is negative—warm-prestress effects (Keeney and Bass, 1994; Bryan et al., 1985)—when the crack becomes critical ($K_I/K_{Ic} > 1$ beyond the HAZ estimated toughness curve). At the center of the HAZ, $\dot{K}$ becomes negative shortly after the crack becomes critical. The peak K_I value at the clad/HAZ interface is lower, but $\dot{K}$ is positive, increasing the probability of initiation.

For the 6:1 crack, Fig. 10(b), the peak K_I value is at the clad/HAZ interface. The crack becomes critical at a slightly earlier time than the 2:1 crack and $\dot{K}$ remains positive well beyond the HAZ estimated toughness curve. At the location of the clad/HAZ interface, the peak K_I value for the 6:1 crack is 27 percent higher than the 2:1 crack.

Summary

Thermo-elastic-plastic analyses were carried out for clad cylinder models with 74-mm-deep 2:1 and 6:1 through-clad inner-surface cracks. For the 2:1 crack, the peak K_I values occurred

at the HAZ/base interface, but $\dot{K}$ is negative when the crack becomes critical. At the center of the HAZ, $\dot{K}$ becomes negative shortly after the crack becomes critical. The peak K_I value at the clad/HAZ interface is lower, but $\dot{K}$ is positive, increasing the probability of initiation. For the 6:1 crack, the peak K_I value is at the clad/HAZ interface. The crack becomes critical at a slightly earlier time than the 2:1 crack and $\dot{K}$ remains positive well beyond the HAZ estimated toughness curve. The analytical results indicate that cleavage initiation is likely to be achieved for the 6:1 crack, but questionable for the 2:1 crack.

References

ABAQUS, 1996, *Theory Manual,* Version 5.5, Hibbit, Karlson and Sorensen, Inc., Providence, RI.

Bass, B. R., 1996, "Report of Foreign Travel of B. R. Bass, Computational Physics and Engineering Division," Lockheed Martin Energy Research Corp., Oak Ridge Natl. Lab., USNRC Foreign Trip Report, ORNL/FTR-5761, Apr.

Bass, B. R., and Bryson, J. W., 1982, "Applications of Energy Release Rate Techniques to Part-Through Cracks in Plates and Cylinders, Vol. 1, ORMGEN-3D: A Finite Element Mesh Generator for 3-Dimensional Crack Geometries," Martin Marietta Energy Systems, Inc., Oak Ridge Natl. Lab., USNRC Report NUREG/CR-2997/V1 (ORNL/TM-8527), Dec.

Bryan, R. H., et al., 1985, "Pressurized-Thermal-Shock Test of 6-in.-Thick Pressure Vessels. PTSE-1: Investigation of Warm Prestressing and Upper-Shelf Arrest," Martin Marietta Energy Systems, Inc., Oak Ridge Natl. Lab., USNRC Report NUREG/CR-4106 (ORNL-6135), Apr.

Keeney, J. A., 1994, "Analysis of Multiple Cracks in the NESC-1 Spinning Cylinder Experiment," Martin Marietta Energy Systems, Inc., Oak Ridge Natl. Lab., USNRC Letter Report ORNL/NRC/LTR-94/35, Dec.

Keeney, J. A., and Bass, B. R., 1997, "Fracture Analysis of the NESC-1 Spinning Cylinder Experiment," ASME JOURNAL OF PRESSURE VESSEL TECHNOLOGY, Vol. 119, pp. 52–56, Feb.

Lacey, D. J., et al., 1991, "AEA Technology, Spinning Cylinder Test 4: An Investigation of Transition Fracture Behavior for Surface Breaking Defects in Thick-Section Steel Specimens," Report AEA TRS 4098, June.

S. McAllister, 1996, "NESC, Minutes of the 7th TG3 Meeting (in combination with TG2)," Framatome, Paris la Défence, NESC DOC TG3 (96)2, May.